IMPLEMENTATION OF A BIOINSPIRED ROBOT (RIVER SALMON) FOR STABILITY CONTROL TROUGH THE DORSAL FIN

[1,2]FAUSTO CABRERA,[3]MARIO ARELLANO, [4]STEVEN GRANIZO, [5]FABRICIO SANTACRUZ [6]CLAUDIO ROSSI

[1] PhD Candidate, Universidad Politécnica de Madrid, Centro de Automática y Robótica UPM-CSIC, Spain

[2,5] Professor, Escuela Superior Politécnica de Chimborazo, Grupo de Investigación en Tecnologías de la

Electrónica y Automatización, Ecuador.

[3,4] Independent Researcher

[6]Full professor, Universidad Politécnica de Madrid, Department of Robotics and Automation, Spain

E-mail: [1]f.cabrera@alumnos.upm.es, [2] fausto.cabrera@espoch.edu.ec, [3] andresmario7@gmail.com, [4]sv_19974@hotmail.com, [5]fabricio.santacruz@espoch.edu.ec, [6] claudio.rossi@upm.es

ABSTRACT

This document shows the stages of design and implementation of a bio-inspired robot in the morphology of an articulated river salmon. This robot imitates the Subcaringiform displacement that the river salmon presents. The principal analysis of the robot was the influence of the dorsal fin during the displacement, the dorsal fin has 2 DOF, in the first stage, a test evaluating the Pitch and Roll movements during the displacement of the robot was determined, in the second stage, we use the movements of the dorsal fin with tests in the same way as in the first stage and the results shown better stability, in the future work a control system in closed loop will be designed in order to obtain desired movements and positions.

Keywords: *bioinspired fish, dorsal fin, subcaringiform, bioinspired robot, stability control.*

1. INTRODUCTION

Bioinspired robots appeared according to F. Zhang, P. Washington, and DA Pal two decades ago, great efforts have been made to design and develop biologically inspired fish robots to improve the performance of existing underwater vehicles. [1] [2].

Various underwater tasks are carried out by manned and unmanned underwater vehicles, aquatic exploration in various research sectors requires increasingly specific equipment and better performance, conventional underwater vehicles have limitations mainly due to their maneuverability, the study of new systems of propulsion and navigation seek to evolve in terms of underwater locomotion, focusing the study on mechanisms that emulate biological beings, in this particular case fish, which have evolved by adapting to the environment and interacting efficiently with the environment.

Research related to fish robots is mainly based on control, autonomy, locomotion, focusing mainly on the caudal, dorsal, and anal fin, which affects the movement and stability of the robot [3].

Currently, bioinspired prototypes make tours of aqueduct tunnels looking for defects in the structures of hydroelectric power plants, oil pipelines, underground gas platforms, such as the "Luma" robot, which was developed and built-in coordination with the programs. of engineering graduate from the Federal University of Rio de Janeiro for Ampla, a company that distributes electrical energy [4]

The fish robot has been theme of research work, due to the complex but useful propulsion system in underwater vehicles, being the caudal fin and a little bit the pectoral fins the focus of attention, let in the second plane the other fins, that offer to the fishes a good maneuverability and interaction in underwater places.

The objective of this research is to control the warping orientation by means of the dorsal fin of a bioinspired robot in a river salmon.

The second chapter shows the methodology related in its entirety to the study of the dorsal fin in a river salmon. The third chapter presents the implementation of the bioinspired robot, giving way to the fourth chapter in which several stabilization tests are presented using the dorsal fin, finally the results, conclusions and recommendations are presented, thus evidencing the operation of the robot through the results of the implementation.

2. METHODOLOGY

The set of fins present in fish has locomotion as its primary objective, the dorsal fins protect the fish from rolling and support it in turns and sudden stops, the present research seeks to stabilize the robot to prevent it from turning on itself.

The minimum size of the dorsal fin in salmon fish is 9 to 10 mm until reaching a definitive number in its growth of 0.26 to 30mm [5] The dorsal fin in salmon fish is made up of membranous structures, which are supported by rays of bone or cartilaginous origin. [6]

2.1 Propulsion systems

Fish locomotion is based on two factors, the first in the form of body movement (wave and oscillatory) and the second in the structure or segments of the fins (propulsion). [14,15]. In figure 1 you can see the parts of the fish involved in its movement.
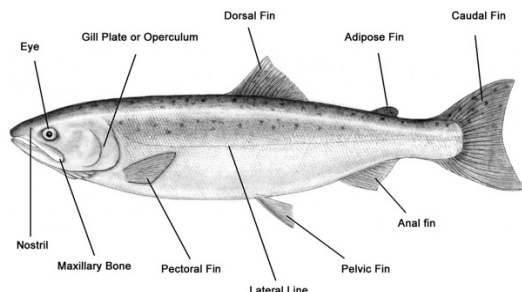

Figure 1: Fins used in the movement of a fish.

The movement is undulatory when the movement is made with the whole body from the head to the tail, while in the oscillatory movement the propulsion occurs mainly in the tail. [18] Inf Figure 2 shows the block diagram of the drive.
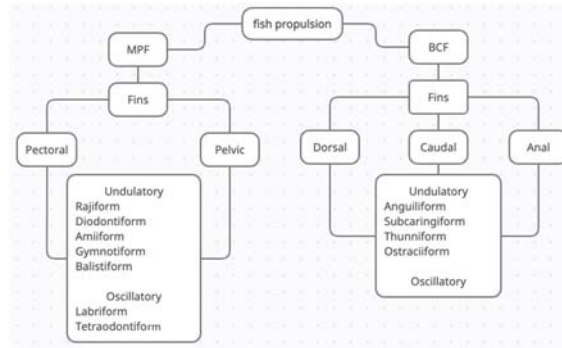

Figure 2: Diagram of fish propulsion mechanisms

The river salmon that has been selected for the present investigation, presents a subcaringiform BFC, in Figure 3 the different types of swimming.
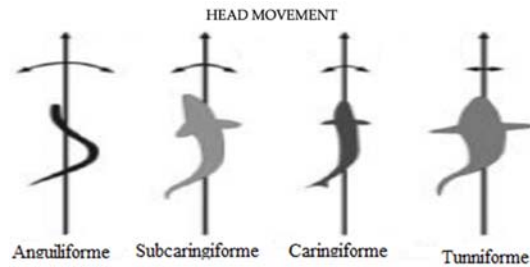

Figure 3: Types of BCF swimming movements

In Subcaringiform swimming mode, significant lateral movements occur only in the caudal fin (which produces more than 90% of the thrust) and in the narrow peduncle [14]. Less musculature is used than in the Eel type. Between a half and two-thirds of muscle mass are used to generate waves throughout the body. To make the Subcaringiform mode like the bioinspired robot for river salmon, 2 mobile links powered by servo motors will be used.

2.2 Stabilization system

Fish interact in underwater environments using their fins (Figure 4), in the particular case of river salmon, the caudal fin provides the animal with the propulsion necessary to move, while the pectoral, caudal, dorsal, and anal fins provide stability.

The fins have been found to generate various wake vortices and fluid forces producing a hydrodynamic interaction with which the fish can maneuver during locomotion.

There are two movements of the dorsal fin, the first refers to a contraction, in which the fin joins the body avoiding any influence during the

movement, this movement occurs when the fish travels at speed on long trajectories, the second movement occurs when the fish needs to maneuver, the pectoral fin rotates in roll producing forces that help the fish to make these sudden movements.
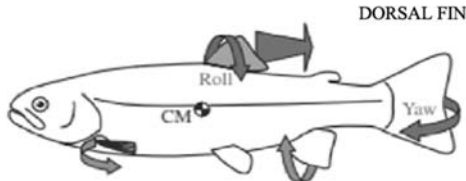

Figure 4: Fins used in the movement of a fish.

The movements of the dorsal fin, therefore, are part of a whole system of locomotion, its movements provide the system with stability to maintain proper orientation in a small instant of time.

Some studies indicate that the soft dorsal fin is not simply passive but can serve as an active control surface. During rapid and stable swimming in fish, the onset of dorsal tilting activity is like that of the ipsilateral red monomeric muscle in a corresponding longitudinal position.

Jayne et al. (Jayne et al., 1996) suggest that such dorsal tipper activation can serve to stiffen the soft dorsal fin and resist its tendency to passively bend as the body sweeps laterally through the water. The idea that movement of the soft dorsal fin is not completely independent of body flexion during stable swimming is supported by two study findings: (i) dorsal fin ripple is observed only when ripple occurs axial and (ii) above the gait transition velocity, the soft dorsal and caudal fins exhibit nearly identical periods of oscillation. [9]

2.3 Kinematic

The study of the dorsal fin is governed under two degrees of freedom with which it will have a position, speed, and acceleration of the fixed link, that is, there is a single movable joint governed by an actuator which in this case is given using an SG90 micro servo motor.

The previous study of direct kinematics allows determining the position and orientation of the dorsal fin concerning a known coordinate system, the geometric parameters of the fish robot.

The position of the dorsal fin is determined by the angular variables of X, Y, Z that can later be achieved using the respective sensor. It should be noted that the position of the second joint is a fixed

value that will always be concerning the position of the first joint. Distances are anatomically visible and referenced to the center of mass of the moving parts of the dorsal fin.

A reference system is established as shown in the buoyancy laws that can be observed below (Figure 5), for the study the Denavit Hartemberg parameters were determined with the consideration of their respective positions.
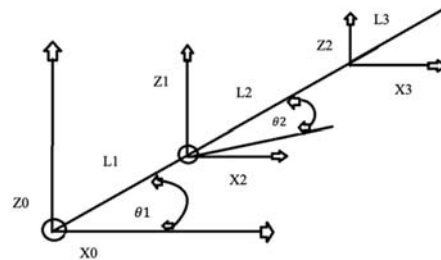

Figure 5: Articular plane of the dorsal fin

$$x_1 = l_1 \cos \theta_1 \qquad (1)$$
$$y_1 = l_1 \sin \theta_1 \qquad (2)$$
$$x_2 = l_2 \cos \theta_2 \qquad (3)$$
$$y_2 = l_2 \sin \theta_2 \qquad (4)$$

Table 1: DH parameters for direct dorsal fin kinematics

θ	D	TO	α
θ1	0	l1	0
θ1	0	l2	0

Through the analytical development of Denavit Hartemberg (Table I), the homogeneous transformation matrix shown below is determined.

$$^0A_2 = \begin{bmatrix} \cos(\theta_1 + \theta_2) & -\sin(\theta_1 + \theta_2) & 0 & l_1\cos\theta_1 + l_2\cos(\theta_1 + \theta_2) \\ \sin(\theta_1 + \theta_2) & \cos(\theta_1 + \theta_2) & 0 & l_1\cos\theta_1 + l_2\cos(\theta_1 + \theta_2) \\ 0 & 0 & 1 & 0 \\ 0 & 0 & 0 & 1 \end{bmatrix}$$

On the other hand, the preliminary study must contain the development of the inverse kinematics of the fish robot whose objective is to find the values that the joint coordinates corresponding to the dorsal fin of the fish robot must take so that its end is positioned and oriented according to a certain location space.

By the aforementioned, the two articular positions of the fish robot for the dorsal fin were determined considering the following parameters.

$$\sigma = \tan^{-1}\left(\frac{y}{x}\right) \tag{5}$$

Where is the angle of the slope of the end effector, that is, the angle of the position where the end effector is located. For ease of calculation, an R variable is estimated that contains information regarding the position and orientation of the end of the fish robot.

$$R^2 = l_1^2 + l_2^2 - 2\cos\varphi \tag{6}$$

The angular positions when performing inverse kinematics at the end of the dorsal fin of the river salmon robot correspond to the following equations, taking into account the aforementioned that the angular position θ2 is always referred to the position θ1.

$$\theta_1 = \sigma - \cos^{-1}\left(\frac{l_1^2 - l_2^2 + R^2}{2Rl_1}\right) \tag{7}$$

$$\theta_2 = \cos^{-1}\left(\frac{-l_1^2 - l_2^2 + R^2}{2l_2l_1}\right) \tag{8}$$

With these previous studies, it will be possible to establish the direction of the movement of the dorsal fin for the direction of the river salmon robot fish.

2.4 Dynamic

Newton Euler's computational algorithm was used for motor sizing:

$$\tau = B(q)\ddot{q} + V(q,\dot{q}) + G(q) \tag{9}$$

Where:

$$w_i = w_{i-1} + Z_{i-1}\dot{q}_i \tag{10}$$

So, the absolute linear speed of the coordinate system linked to each link is calculated as:

$$v_i = w_i \times P_i^* + v_{i-1} \tag{11}$$

Acceleration is calculated as:

$$\dot{v}_i = \dot{w}_i \times P_i^* + w_i \times (w_i \times P_i^*) + \dot{v}_{i-1} \tag{12}$$

Where:

$$F_i = \frac{d(m_i\bar{v}_i)}{dt} = m_i\bar{a}_i \tag{13}$$

$$N_i = \frac{d(I_iw_i)}{dt} = I_i\dot{w}_i + w_i \times (I_iw_i) \tag{14}$$

$$f_i = f_i - f_{i+1} \tag{15}$$

$$n_i = n_{i+1} + P_i^* \times f_{i+1} + (P_i^* + \bar{S}_i) \times F_i + N_i \tag{16}$$

It is observed that these equations are recursive and allow obtaining the forces and moments in the elements i = 1, 2 ..., n for a robot with n elements. and represent the force and momentum exerted by the robot fish's motor on an external object. f_{i+1} n_{i+1}

Therefore, the torque/force for each joint is expressed as

$$\tau_i = n_i^T z_{i-1} + b_i\dot{q}_i \tag{17}$$

Where is the viscous coefficient of friction of the joint b_i.

Using these data, the Newton Euler method is applied to obtain the desired torque for the motor.

From the inverse dynamics, the amount of torque that we need to carry out the movement is determined, with this information the type of servomotor that we require for the implementation of the fish robot, which is the SG90 micro servo, was determined.
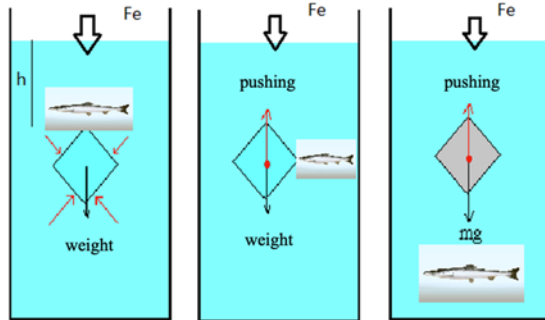
2.5 Floatability

Figure 6: Buoyancy principle of a solid body

For experimentation in the operation of the robot, the disposition of the water at rest is required, which leads to a physical variable called hydrostatics and the pressure exerted under these conditions. Hydrostatic pressure is applied to a static and incompressible flow point.

In figure 6 a body (fish) submerged in water is observed, in which the forces involved for its buoyancy have been described, according to the Archimedean principle [20]. Where:

The summation of forces is performed to determine the external force (Fe) necessary to keep the bioinspired robot in balance and completely submerged.

$$F_e = M_{agua\ desalojada} \times g \tag{18}$$

$$F_e = V_{sumergido} \times d_{agua} \times g \tag{19}$$

The guarantees of the study require the consideration of the buoyancy height using the following equation.

$$F_e = (S \times h) \times d_{agua} \times g \tag{20}$$

There S is the surface of the rigid body (robot fish) and h the height between the water level and the upper limit of the fish.

$$F_e = (S \times 0.01m) \times 997\frac{kg}{m^3} \times 9.81\frac{m}{s^2} \tag{21}$$

$$F_e = 132.35\ N \tag{22}$$

Once the thrust force of the water is determined, the necessary weight for the buoyancy of the robot in the water is established.

Being an irregular rigid body the best way to determine the volume is through experimentation, that is, immersing the body in a container full of water, the difference between the full container and the new amount of water will correspond to the volume of the robot.

3. DESING

The design of a bioinspired robot in a river salmon was carried out in stages using a virtual design tool called Solid Works. This design is presented below, all the data is given in (grams * square millimeters):

Mass = 41.75 grams

X = 0.00

Y = -1.49

Z = -39.65

Ix = (0.00, 0.10, 1.00) Px = 24426.29

Iy = (0.00, -1.00, 0.10) Py = 33183.95

Iz = (1.00, 0.00, 0.00) Pz = 44394.01

Lxx = 44393.99 Lxy = 15.81Lxz = -3.64

Lyx = 15.81 Lyy = 33102.80 Lyz = 839.22

Lzx = -3.64 Lzy = 839.22 Lzz = 24507.46
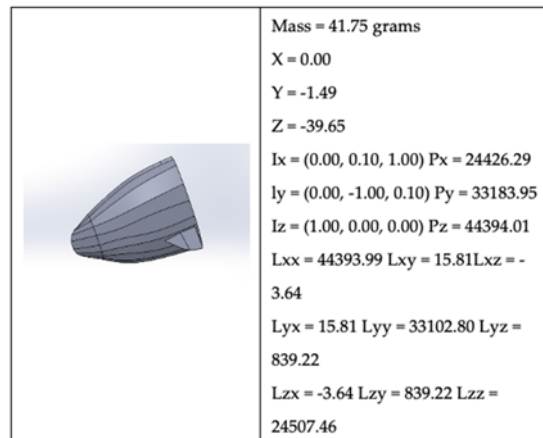
Figure 7: Design of the head of a salmon

3.1 Body and back

Z = -29.29

Ix = (0.00, 1.00, 0.01)

Px = 20309.76

Iy = (0.00, -0.01, 1.00)

Py = 22641.01

Iz = (1.00, 0.00, 0.00)

Pz = 33337.50

Lxx = 33337.50   Lxy = 0.00

Lxz = 0.00

Lyx = 0.00 Lyy = 20309.8

Lyz = 12.31

Lzx = 0.00 Lzy = 12.31

Lzz = 22640.94

Figure 8: Back of the fish

Mass = 45.78 grams

Ix = (0.00, 0.01, 1.00) Px = 17771.77

Iy = (0.00, -1.00, 0.01) Py = 39537.03

Iz = (1.00, 0.00, 0.00) Pz = 50878.09

Lxx = 50878.09   Lxy = 0.40

Lxz = 3.48

Lyx = -0.40 Lyy = 39532.13   Lyz = 326.35

Lzx = 3.48 Lzy = 326.35

Lzz = 17776.67
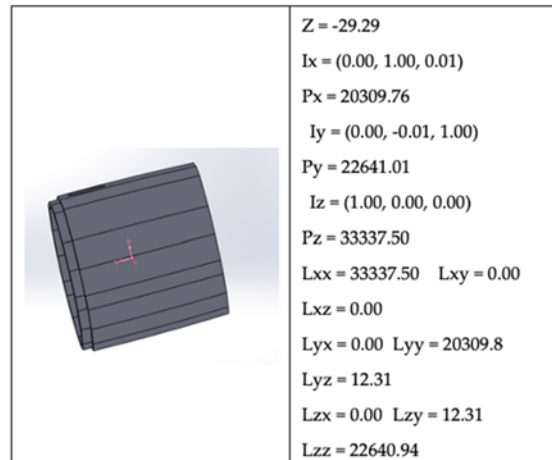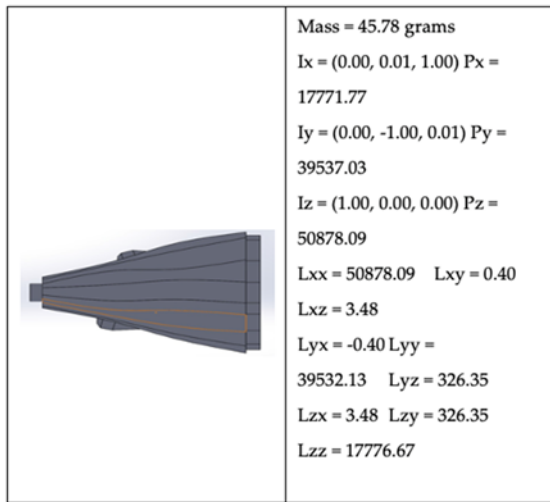
Figure 9: Design of the body of a river salmon next to the pectoral fins

3.2 Caudal fin

Mass = 7.37 grams

X = 0.00

Y = 1.17

Z = -23.32

Ix = (0.00, 1.00, -0.04)

Px = 947.93

Iy = (0.00, 0.04, 1.00)

Py = 3452.78

Iz = (1.00, 0.00, 0.00)

Pz = 4374.72

Lxx = 4374.72

Lxy = 0.00

Lxz = 0.03

Lyx = 0.00

Lyy = 951.18

Lyz = -90.06

Lzx = 0.03

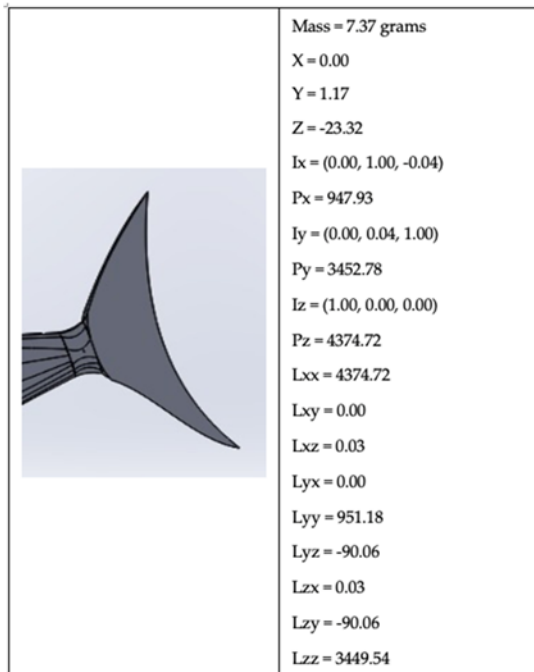Lzy = -90.06

Lzz = 3449.54

Figure 10: Design of the caudal fin of a river salmon

3.3 Dorsal fin

The dorsal fin naturally in fish has the main function of stabilizing and orienting the fish according to its size, weight, and type of fish in question, making it very important and indispensable for characterizing fish movements. The design of the dorsal fin was made for two free basses to obtain a more precise movement and similar to a natural fin.

First degree of freedom (auxiliary). Joint movement (120 degrees to the right and 120 degrees to the left from the origin
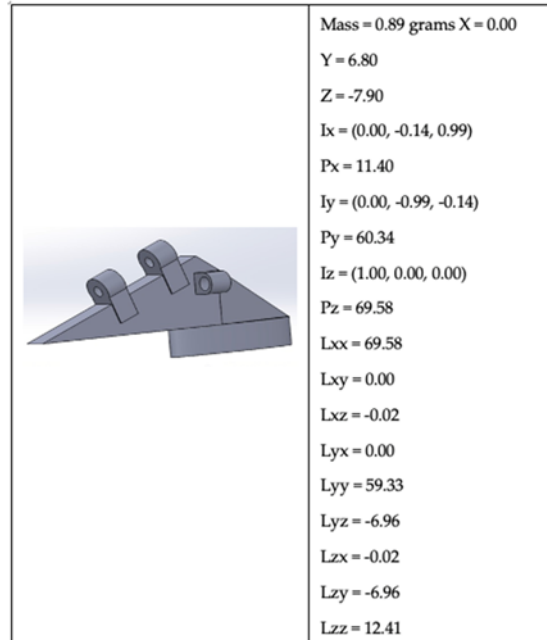
Mass = 0.89 grams X = 0.00

Y = 6.80

Z = -7.90

Ix = (0.00, -0.14, 0.99)

Px = 11.40

Iy = (0.00, -0.99, -0.14)

Py = 60.34

Iz = (1.00, 0.00, 0.00)

Pz = 69.58

Lxx = 69.58

Lxy = 0.00

Lxz = -0.02

Lyx = 0.00

Lyy = 59.33

Lyz = -6.96

Lzx = -0.02

Lzy = -6.96

Lzz = 12.41

Figure 11: Dorsal fin design (1st degree of freedom)

The second degree of freedom. Joint movement (90 degrees to the right and 90 degrees to the left from the origin)

Mass = 0.61 grams X = 1.00

Y = -0.71

Z = -1.86

Ix = (0.00, -0.15, 0.99)

Px = 8.81

Iy = (0.00, -0.99, -0.15)

Py = 23.56

Iz = (1.00, 0.00, 0.00)

Pz = 30.82Lxx = 30.82

Lxy = 0.00Lxz = 0.00

Lyx = 0.00

Lyy = 23.20Lyz = -2.25
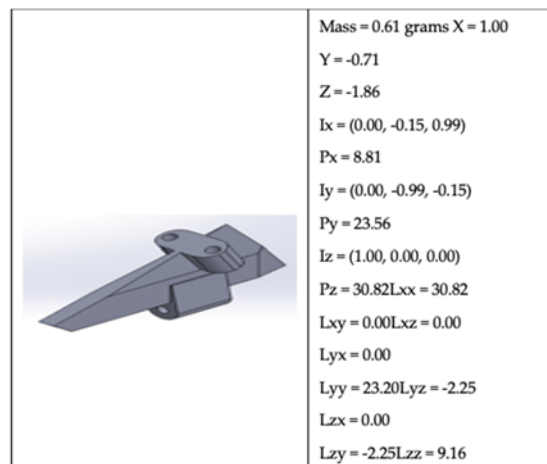
Lzx = 0.00

Lzy = -2.25Lzz = 9.16

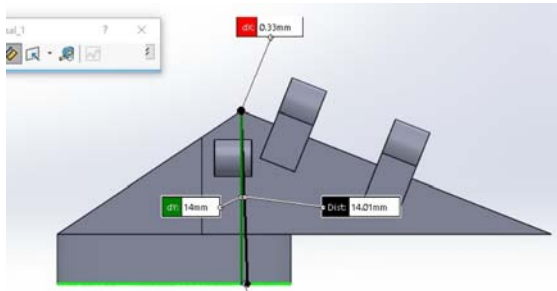*Figure 12: Dorsal fin design (2nd degree of freedom).*

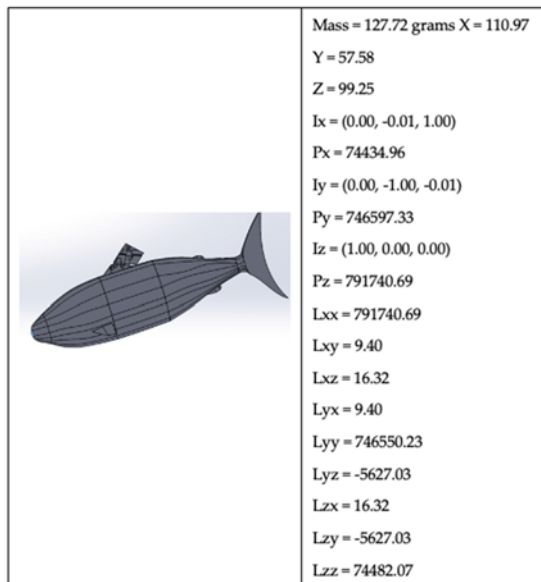*Figure 13: Dorsal fin design with its dimensions*

3.4 Whole-body

Figure 14: Complete design of the bioinspired robot in a river salmon on a SolidWorks platform

Robot implementation together with electronic devices
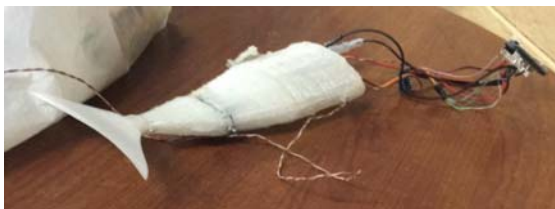

Figure 15: A printed robot, bioinspired in river salmon, along with electronic devices

Waterproofing of electronic elements, with the aim of correct operation underwater. First, the physical modeling of the salmon fish was performed in SolidWorks as detailed above, and then it was 3D printed. Then, with the help of an Arduino nano, programming was developed to characterize the movement and function of a dorsal fin, which constantly receives data from an IMU inertial measurement unit to correct the position and orientation errors of the prototype to maintain it in a vertical (90 degrees) steadily.

The movement of the fin was carried out using an SG90 servo motor, which allows us to make precise movements through gradual movements made by programming. Below is the servo motor used:

- ✓ Equipment and Materials Used
- ✓ Arduino Nano
- ✓ MPU6050
- ✓ SG90 Servomotors
- ✓ Lipo Battery 7V
- ✓ Connection cables

Later, it was externally waterproofed with a waterproof material, called hypoxic resin, as well as a malt was used to completely mold the salmon fish and give it its characteristic color, then it is presented in the image to the prototype swimming and running tests:

Figure 16: Bio robot inspired by a river salmon undergoing functional tests in a swimming pool.

4. ANALYSIS AND RESULTS

19 tests were taken in 6 different positions to estimate the stabilization time. The prototype was placed at a certain degree of inclination, and the time it took to return to the set point was measured.

We also add a box and mustache graph to each test to show where the data is grouped. Considering that we refer to the time it takes to get to the SP.

Table 2: Summary of average prototype stabilization times

Degrees	Average stabilization time in seconds.
90	4
75	3
Four. Five	2
-90	4
-75	3.5
-Four. Five	2

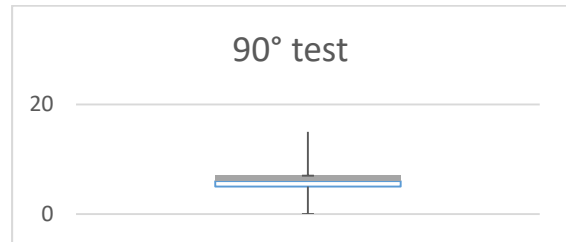*Figure 17: Data grouping at 90 °(time to set point return).*

Table 3: Stabilization tests al 90°

DEGREES	Time for Stabilization
90	7
90	6
90	7
90	7
90	6
90	6
90	5
90	12
90	15
90	5
90	6
90	7
90	6
90	7
90	13
90	7
90	7
90	5
90	7

Table 6: Stabilization Tests at 75 °

Degrees	Time for ST
75	5
75	4
75	5
75	5
75	5
75	4
75	4
75	4.5
75	8
75	7
75	4.5
75	5
75	4.5
75	5
75	7
75	9
75	5
75	5.5

Table 7: Min, max and quartiles of tests at 75 °

	VALUE	Width
MIN	4	4
Q1	4.5	0.5
Q2 (AVERAGE)	**5**	**0.5**
Q3	5,375	0.375
MAX	9	3,625

Table 4: Values min, max, and 90° test quartiles

	VALUE	Width
MIN	5	5
Q1	6	1
Q2 (MEDIUM)	**7**	**1**
Q3	7	0
MAX	15	8

Table 8: Inter quartile, min, and max value to determine that all values are typical of tests at 75 °

RIC	0.875
VAL. MIN	2,625
VAL. MAX	6.015625

Table 5: Interquartile range, value min, and max to determine that all values are typical.

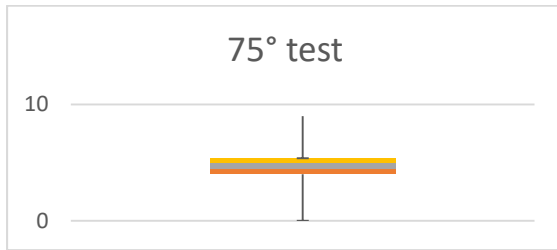| RIC	1
VAL. MIN	4.5
VAL. MAX	8.5

Figure 18: Grouping data at 75 °(time to set point return).
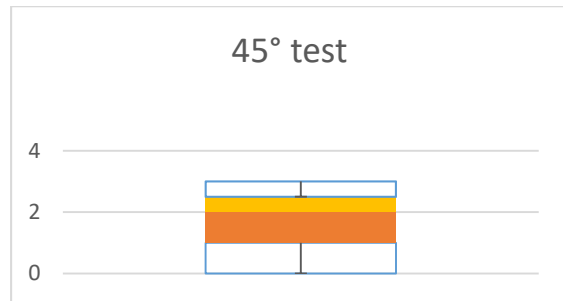
Figure 19: Data grouping at 45 °(time to set point return).

Table 9: Stabilization at 45°

Degrees	Time for ST
45	3
45	3
45	2.5
45	3
45	3
45	4
45	3.5
45	4
45	7
45	3
45	3
45	3
45	3
45	3.5
45	2.5
45	3.5
45	3
45	3

Table 10: Min, max and quartiles test values at 45 °

	VALUE	Width
MIN	1	1
Q1	2	1
Q2	**2**	**0**
Q3	2.5	0.5
MAX	3	0.5

Table 11: Interquartile range, min and max value to determine that all values are typical of tests at 45 °

RIC	0.5
VAL. MIN	0.75
VAL. MAX	2.5

Table 12: Stabilization at -90 °

Position -90	Time for ST
-90	8
-90	9
-90	9
-90	9
-90	8
-90	9
-90	9
-90	8
-90	9
-90	8
-90	9
-90	11
-90	12
-90	9
-90	7
-90	8
-90	9
-90	8

Table 13: Values min, max. and test quartiles at -90 °

	VALUE	Width
MIN	3	3
Q1	4	1
Q2 AVERAGE	**4**	**0**
Q3	5	1
MAX	5	0

Table 14: Interquartile range, min, and max value. to determine that all values are typical of 45 ° tests.
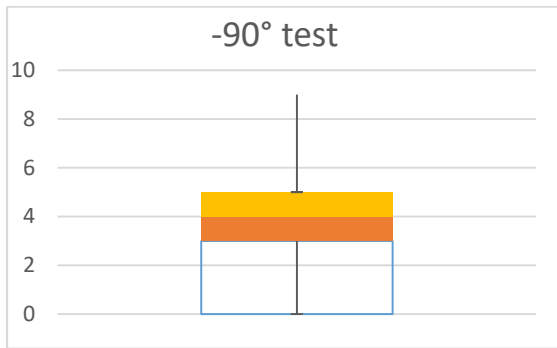
RIC	1
MIN	2.5

MAX	6.5

Figure 20: Grouping data at -90 °(time to set point return).

Table 15: Stabilization -75 °

Time -75	Time for ST
-75	6
-75	6
-75	5
-75	6
-75	6
-75	5
-75	8
-75	6
-75	6
-75	6
-75	5
-75	5
-75	5
-75	6
-75	5
-75	6
-75	7
-75	6

Table 16: Min, max and test quartiles values at -75 °

	VALUE	Width
MIN	5	5
Q1	5	0
Q2 (AVERAGE)	**6**	**1**
Q3	6	0
MAX	8	2

Table 17: Interquartile range, min, and max value. to determine that all values are typical of tests at -75 °

RIC	1
MIN	3.5
MAX	7.5

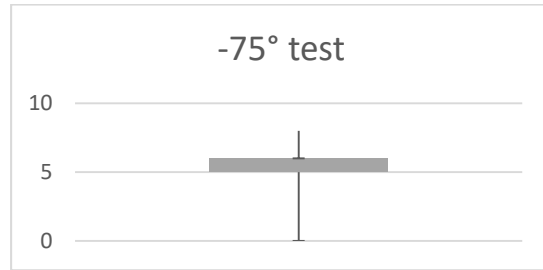*Figure 21: Data grouping at -75 ° (time to set point return).*

Table 18: Stabilization at -45 °

Even time -45	Time for ST
-45	3
-45	2
-45	3
-45	3
-45	4
-45	5
-45	3
-45	2
-45	2
-45	2
-45	3
-45	3
-45	3
-45	3
-45	4
-45	2
-45	4
-45	3

Table 19: Min values, max. and test quartiles at -45 °

	VALUE	Width
MIN	2	2
Q1	2.25	0.25
Q2 (AVERAGE)	**3**	**0.75**
Q3	3	0
MAX	5	2

Table 20: Interquartile range, min, and max value. to determine that all values are typical of tests at -75 °

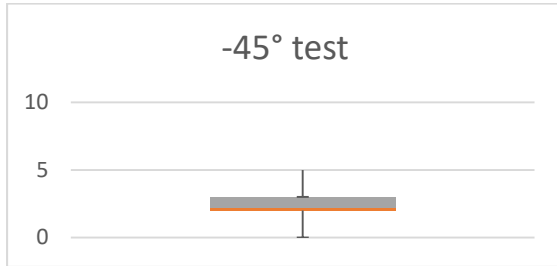| RIC	0.75
MIN	0.5625
MAX	3,375

Figure 22: Data grouping at -45 °(time to set point return).

4.1 Gaussian bell on individual results

In the following section, we group all the tests to different degrees and their return time to SP, to organize in a gauss bell and show how the return times to ST are grouped.

Table 21: Data to carry out the Gaussian bell.

Position	Medium
-90	**4**
-75	3.5
-45	2
45	2
75	3
90	4

Average	deviation	max.	min
3.083333333	0.91742393	4	2

Figure 23: Gauss bell returns to setpoint.

Table 22: Normal Time Distribution to SP

	DISTRIB
1	0.033003695
1.3	0.065741372
1.6	0.117672654
1.9	0.18926614
2.2	0.27354633
2.5	0.355262568
2.8	0.414599332
3.1	0.434778777
3.4	0.409702547
3.7	0.346920195
4	0.263967883
4.3	0.180481706
4.6	0.110885785
4.9	0.061218002
5.2	0.030369876
5.5	0.013538404
5.8	0.005423161
6.1	0.001952082

Next, the positions that are obtained from the fish as it moves in real-time are detailed, as well as the positions that are obtained through the application developed to monitor said movements.

Table 23: Set Values vs obtained through software.

Values setpoint		IMU measurement position	
Pitch	Roll	Pitch	Roll
1	2. 3	2	22
7	24	5	2. 3
10	24	9	25
18	24	17	25
2. 3	2. 3	22	22
22	2. 3	24	24
32	2. 3	30	24
32	24	3. 4	25
36	2. 3	39	24
42	2. 3	45	24

After obtaining the respective positions of both the IMU and those obtained through the mobile application, a comparison will be made to obtain the percentage of error in said measurements, said table

is detailed below, where it was determined that the error latency is from ± 5%

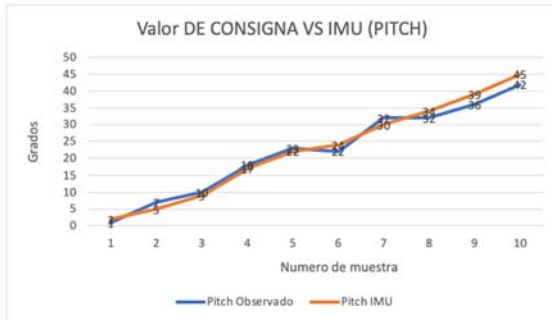*Figure 24: Comparison of the error around the PITCH.*

Figure 25: Comparison of the error around ROLL

Table 24: Percentage of error in percentage obtained in the pitch and roll position measurements observed vs those obtained by software.

Error	
Roll error	Pitch error
4.55%	0.00%
4.35%	3.44%
4.00%	4.50%
4.00%	5.88%
4.55%	4.55%
4.17%	8.33%
4.17%	6.67%
4.00%	5.88%
4.17%	7.69%
4.17%	6.67%

5. CONCLUSIONS

A robot inspired by a salmon fish was designed, it can maneuver and move in underwater places, the actuators were sized based on establishing the dynamics of the robot, it was calculated to in a non-underwater environment, in order to make the joint move underwater, the actuator was oversized. Once the actuator was selected, the design was completed, and the robot was built. Various methods were carried out for waterproofing the electronics and actuators, finally achieving underwater operation, various designs were used to obtain zero buoyancy, but none worked properly, a nylon cord was used to maintain the fish robot submerged in a constant deep, Thus, it proceeded to perform the functional tests.

Several tests were applied to the robot in search of identifying the action performed by the dorsal fin in terms of the stability of the robot in warping, the results showed that the dorsal fin exerts an effect and collaborates with the maneuverability of the robot, the pitch and roll errors of the test using the dorsal fin are less than the results without the action of this.

This research begins with the analysis of the dorsal fin, with some results that shown improvement in the maneuverability of the robot, in the future it would be interesting to apply control systems to obtain desired movements using the dorsal fin.

REFRENCES:

[1] C. Rodriguez, "Prototype of an underwater robot with the ability to track trajectories using image processing," *Univ. Pedagógica Nac.*, 2014.

[2] P. Zhang, "A Flexible, Reaction-Wheel-Driven Fish Robot: Flow Sensing and Flow-Relative Control", pp. 1221–1226, 2016., "pp. 1221–1226, 2016.

[3] Lindsey, C. C. (1978). Form, function, and locomotory habits in fish. In Fish Physiology (Vol. 7, Issue C). https://doi.org/10.1016/S1546-5098(08)60163-6.

[4] Yan, Q., Wu, W. G., Zhang, S. W., Xu, M., & Yang, J. (2009). Preliminary study of flexible pectoral fin capable of 3D motions actuated by shape memory alloy. 2009 IEEE International Conference on Robotics and Biomimetics, ROBIO 2009, 1814–1819.

https://doi.org/10.1109/ROBIO.2009.5420557.

[5] H. Hernández and M. Rojas, "Development of the salmon spinal cord (Salmo salar) during the post-hatching period," *Int. J. Morphol.*, vol. 31, no. 1, pp. 172–176, Mar. 2013.

[6] Sfakiotakis, M., Lane, D. M., & Davies, J. B. C. (1999). Fish Swimming Techniques. Journal of Oceanic Engineering, 24(2), 237–252. file:///Z:/Commercial/Current_Projects/14001/Research_Literature/Fish_Swimming_Techniques.pdf.

[7] EG Drucker and GV Lauder, "Locomotor function of the dorsal fin in rainbow trout: Kinematic patterns and hydrodynamic forces," *J. Exp. Biol.*, vol. 208, no. 23, pp. 4479–4494, 2005.

[8] Wang, W., Dai, X., Li, L., Gheneti, B. H., Ding, Y., Yu, J., & Xie, G. (2018). Three-Dimensional Modeling of a Fin-Actuated Robotic Fish with Multimodal Swimming. IEEE/ASME Transactions on Mechatronics, 23(4), 1641–1652. https://doi.org/10.1109/TMECH.2018.2848220.

[9] EG Drucker and GV Lauder, "Locomotor function of the dorsal fin in teleost fishes: Experimental analysis of wake forces in sunfish," *J. Exp. Biol.*, vol. 204, no. 17, pp. 2943–2958, 2001.